Geographic variation in vulnerability to warming temperatures in an intertidal barnacle species.

Short title: Geographic variation in vulnerability to warming

Sarah E. Gilman[1*], Gordon T. Ober[1,#a], Rhiannon L. Rognstad[1], Madeleine Bunnenberg-Ross[2], and Tingyue Man[2]

[1]W. M. Keck Science Department of Scripps, Pitzer, and Claremont McKenna Colleges, Claremont , CA USA

[2]Pitzer College, Claremont, CA USA

[#a]Current Address: Environmental Science Department, Endicott College, Beverly, MA USA

[#b]Current Address: Data Lab, World Resources Institute, Washington DC, USA

*Corresponding author

E-mail: sgilman@natsci.claremont.edu (SEG)

Abstract

For most species, we lack a detailed understanding of how vulnerability to warming temperatures under climate change varies across a its geographic distribution. Vulnerability arises when there is a gap between local climate and local physiology. Intertidal species are unique because they face two distinct thermal environments, and it is unclear which is the bigger driver of thermal physiology and vulnerability. Here we compare the thermal environments and physiology of three populations of the intertidal barnacle *Balanus glandula*, spanning 1460 km of its geographic range. We measured energy consumption in the laboratory across a 5-hour emersion and subsequent 6-hour immersion at 7 different emersion temperatures. We compared these results to one year of emersion and immersion temperature data from each location. Our results suggest that the temperatures experienced during emersion are a bigger driver of each population's thermal physiology than those experienced during immersion. We also estimated vulnerability to future warming in two ways: by calculating the total energy consumption over a year and by calculating the number of days that temperature exceeded each population's thermal peak. These produced conflicting results. The central population spent the most days over its thermal peak, but the northernmost population had the greatest total costs over a year. This difference may be explained in part by a strong latitudinal gradient in primary productivity that selects for higher energy demand in higher latitude populations. Thus, accurate predictions of B. glandula's response to warming temperatures will require knowledge of both future temperature and food availability.

Introduction

Identifying the species, and populations within species, most vulnerable to warming temperatures under climate change is a pressing goal of ecology [1,2]. A population's vulnerability is determined by the magnitude of expected warming relative to its current thermal physiology and to its capacity to alter its physiology through genetic adaptation or phenotypic plasticity. Populations from different locations within a species' geographic range don't experience the same temperatures [3,4], unlikely to experience the same amounts of warming [5], and likely exhibit different degrees of local adaptation and thermal plasticity [6,7]. This is particularly true for ectotherms, whose body temperatures reflect a complex interaction between the individual organism and its environment [8–10]. While several theories predict how vulnerability to warming should vary across a species range [2,11], our understanding is constrained by a limited number of empirical studies [2]. Without information for a wide range of species and habitats, it will be difficult to accurately predict and ameliorate vulnerabilities to climate change.

Hayford et al. [10] distinguish two general approaches to assessing a population's vulnerability to warming under climate change. Discrete or threshold approaches [e.g., 2,11,12] focus on identifying the frequency of exposure to a threshold temperature above which organisms experience thermal stress and/or death. Populations that spend more time over such a threshold, either currently or under predicted future temperatures, are considered more vulnerable to warming. Threshold temperatures are usually identified from a thermal performance curve ("TPC", Fig 1) of a trait related to fitness. Commonly used thresholds include the critical thermal maximum and lethal limit [13], but the peak of the thermal performance curve ("T_{peak}", also known as the thermal optimum) may be more relevant physiologically

64 [12,14] and easier to accurately estimate [15]. Continuous approaches [12,16] calculate the full
65 energetic cost of exposure to a continuous time series of temperatures for either current or future
66 climates at that location. Populations that show higher total costs under those current or future
67 temperatures are predicted to be more vulnerable to warming. Costs are usually estimated from a
68 TPC curve fitted for oxygen consumption [16,17], with the assumption that costs continue to
69 increase above T_{peak} (Fig. 1) [18]. Costs can also be incorporated into more detailed energetic
70 models that predict growth rates and/or energy balance [19,20], although this requires knowledge
71 of food availability and intake rates, both of which also may change with warming temperatures
72 [21]. Of the two, the threshold approach is more commonly used because it requires less detailed
73 information, but it has also been criticized for that lack of detail [12]. It is not known if the two
74 approaches produce similar predictions.
75
76 **Figure 1. Stereotypical patterns of thermal performance and energetic cost for a**
77 **poikilotherm.** For most traits (solid line), performance increases up to a peak beyond which it
78 decreases. Further warming can lead to reversible (CT_{max}) and irreversible (LT_{max}) loss of
79 function. Energetic costs of exposure to temperature (dashed line) are usually estimated from a
80 TPC curve for metabolic rate or respiration, with the assumption that the full cost of exposure
81 continues to increase exponentially above T_{peak}, even as organism function declines. Figure
82 modified from Hayford et al. [10].
83
84 Intertidal habitats present additional challenges to, and opportunities for, understanding
85 biogeographic variation in thermal physiology. Intertidal organisms alternate between terrestrial
86 and marine conditions with the daily oscillation of the tides, each with a distinct thermal

87 environment. Because terrestrial climates are more variable and exhibit greater thermal extremes
88 than marine climates, we would expect the two environments to select for very different
89 physiologies. It is generally unknown which of the two environments is the bigger driver of an
90 intertidal organism's thermal physiology. Many intertidal species are active mainly when
91 immersed and minimize activity and metabolism during low tide [22,23]. Thus natural selection
92 might favor a thermal physiology that is closely matched to the aquatic thermal environment
93 [24,25]. But intertidal species experience their greatest thermal extremes during emersion and
94 must survive and maintain some metabolic function during those times. Therefore natural
95 selection could also favor physiologies that enhance tolerance and/or performance during
96 emersion. Indeed high shore intertidal species frequently exhibit greater thermal tolerances than
97 their lower shore congeners, despite experiencing the same aquatic thermal environments [26].
98 This latter pattern is predicted by the Climate Extremes and Climate Variability Hypotheses
99 (CEH/CVH), which argue that species, or populations within species, experiencing greater
100 thermal variability should have broader thermal tolerances [27].
101 Approximately 60% of the world's coastlines experience diurnal or mixed semi-diurnal
102 tides [28]. In these tidal regimes, aerial exposure is concentrated in a single low or lower-low
103 tide, the timing of which may vary with season, latitude, and coastal geomorphology [29]. The
104 timing of this low tide can decouple emersion temperatures from latitudinal gradients in
105 terrestrial climate, by filtering the time of day that organisms are exposed to terrestrial climate
106 [3,30]. For example, in the northeastern Pacific, intertidal sites at higher latitudes in Oregon and
107 Washington are much more likely to be exposed to air in middle of the day during the summer
108 than lower latitude locations in California, but the opposite is true in winter (Fig 2B). This
109 difference in the timing of the lower low tide creates thermal hotspots – high latitude locations

110 that experience greater daily maximum temperatures than lower latitude locations, despite have a
111 cooler terrestrial climate overall [3,30]. This decoupling of emersion and immersion thermal
112 regimes creates a unique opportunity to ask which environment is more important in driving
113 thermal physiology and potentially test predictions of the CEH/CVH, which have not explicitly
114 been tested in intertidal species [27]. However, past studies of thermal physiology of NE Pacific
115 intertidal species provide conflicting results. While strong physiological differences have been
116 identified between populations north and south of a known biogeographic break at Pt.
117 Conception, CA (Fig 2A) [e.g., 31]; intraspecific comparisons at higher latitudes have variously
118 shown associations with low tide temperatures [32], water temperatures [33], or no
119 differentiation at all [34].
120
121 **Figure 2. Location of the three populations used in this study (A) and representative**
122 **summer and winter spring tides for the sites (B).** The double-ended arrow in (A) indicates the
123 geographic distribution of *B. glandula*, which extends from Mexico to Alaska [35]. The flat-
124 headed arrow indicates the region of genetic sampling in Sotka et al. [36] and Wares and Skozen
125 [37], with the genetic cline indicted by the dashed portion. "PC" indicates the thermal break at
126 Point Conception, California. The predicted tides in (B) for June 15, 2022 ("Summer") and
127 December 23, 2002 ("Winter") were calculated using the xtide program
128 (http://tbone.biol.sc.edu/tide/index.html)
129
130 Here we extend an earlier study of the thermal physiology of the barnacle *Balanus*
131 *glandula* from single a high latitude northeastern Pacific population [38] to two additional sites
132 spanning 1460 km (Fig 2A) to address two specific research questions: 1) Is terrestrial or marine

133 climate the stronger driver of thermal physiology? and 2) which population is most vulnerable to
134 warming temperatures under climate change? *Balanus glandula* is a common mid to high shore
135 barnacle along the Pacific Coast of North America from Mexico to Alaska [35]. It has also been
136 introduced to Asia, Africa, and South America [39,40]. For each study population, we measured
137 respiration over a 5-hour emersion and a subsequent 6-hour immersion at 7 different emersion
138 temperatures. We compare these results to intertidal and water temperature data collected for one
139 year at each study site.

140 Based on previous studies [3,30,41], we expected the aquatic thermal environments of
141 these three sites to correlate with latitude, but the emersion thermal regimes to be uncorrelated.
142 Specifically, we expected the southernmost site, Newport Bay (hereafter referred to as SC) to
143 have the warmest immersion and emersion conditions, because it occurs south of Point
144 Conception, CA. We expected the northernmost site, Friday Harbor (hereafter referred to as FH)
145 to have the coldest immersion thermal regime, but an intermediate emersion thermal regime
146 because it had previously been identified as a high latitude hotspot [3]. These three sites also
147 span a known genetic cline between two mitochondrial genotypes in *Balanus glandula* [37,42].
148 The central site, Bodega Bay (hereafter referred to as BB), occurs in the middle of this cline and
149 the other two sites are beyond its endpoints (Fig 2A). Limited evidence suggests the genetic
150 cline may reflect adaptation to different thermal regimes [37,42].

151 To address our first question, we estimated the thermal performance curve (Fig 1) for
152 each population and tested for differences in the peaks of the curves among populations.
153 Because we expected the FH site to have warmer low tide and cooler aquatic conditions than the
154 BB site, we predicted the FH population would have a warmer thermal peak (T_{peak}) than BB if
155 emersion temperatures influence physiology but the opposite pattern if water temperature is more

important. We also examined temporal patterns of oxygen demand over the duration of individual emersion and immersion trials to identify additional signs of increased energy demand or physiological stress that could signify a thermal threshold. To address ours second question, we calculated a combined TPC across emersion and immersion phases. We used this curve, in combination with local environmental data, to calculate vulnerability in two ways: the number of days in which temperatures exceeded T_{peak} and the total annual cost of low tide exposure for each population at each site.

Methods

Study sites

All three study sites (Fig 2) experience mixed semi-diurnal tidal cycles with two unequal low tides. At all three sites animals were collected inside bays or fjords that were protected from most wave action. At the northern Friday Harbor ("FH") site, we collected barnacles by deploying 15cm x 15cm PVC settlement plates intertidally off the Friday Harbor Labs dock (48.5457°N, 123.0127W). The dock also contained a NOAA monitoring station [43], which records water temperatures every 6 minutes. Intertidal temperature dataloggers were placed on a west-facing rock wall, approximately 100 m from the collection site. Additional details for this site are described in Ober et al. [38]. At the central site in Bodega Bay CA ("BB", 38.3037N, 123.0532°W), barnacles were collected both growing on mussel shells within the bay and on PVC settlement plates attached to a rope hung between pieces of iron rebar [44]. Temperature dataloggers were placed on the northern face of the southern jetty, approximately 500-1000m in between the two collecting sites. Water temperature data for BB came from the CeNOOS Automated Shore Station at Bodega Marine Laboratory [45], approximately 2km away, which

178 records every 6 minutes. At the southern field site (southern California "SC"), barnacles were
179 collected on oyster shells growing on an artificial jetty on the eastern side of the mouth of
180 Alamitos Bay (33.7484N, 118.1155W). Temperature data loggers were placed on a southeast-
181 facing artificial sea wall in Newport Bay (33.6022°N,117.8824°W), approximately 27 km from
182 the collecting site. Water temperature data came from the SCCOS Automated Shore station at
183 Newport Pier [46], approximately 1.7 km from the sea wall.

184 Intertidal temperature measurement

185 Intertidal temperature dataloggers were established at each site as part of separate study
186 of barnacle growth rates in the field (Gilman et al. *in prep*). For this study we used 1 year of data
187 from loggers located in the approximate vertical center of the barnacle zone. The dataloggers
188 were affixed directly to the rock with epoxy and recorded temperature every 15-20 minutes.
189 This method directly mimics barnacle temperatures [41,47], as a large proportion of a barnacle's
190 surface area is in direct contact with the rock. At FH and BB, we used three replicate Tidbit
191 loggers (v1 or v2 Onset Computer Corp., Bourne, MA, USA). At SC, two replicate DS-1921G
192 ibutton dataloggers (Analog Devices Inc., Wilmington MA, USA) were used. Loggers were
193 downloaded and replaced every 6 months at BB and FH and every 2-4 weeks at SC.
194 We calculated daily physiological maxima (DPM) for the intertidal and water temperature
195 datasets as the 97.9 percentile of the daily data, after first selecting the maximum temperature
196 among any replicate dataloggers within each site and timepoint. This percentile reflects a
197 temperature exposure of at least 30 minutes, corresponding to the minimum time threshold for an
198 organism to experience physiological consequences [5,48].

199 ## Animal collection and maintenance

200 As described in Ober et al. [38], collected barnacles were isolated, tagged, and their
201 maximum opercular diameter measured. Barnacles were maintained in the laboratory in a tidally
202 cycling tank with a daily light cycle (Table 1). They were fed brine shrimp (*Artemia spp.*, Pentair
203 Aquatic Eco-Systems, Apopka, FL 32703) two to three times per week [49]. Laboratory tidal
204 regimes (Table 1) were based on local tidal cycles for the warmest part of the year at each site
205 (approximately July-October for SC and BB and April – August for FH), at a height equivalent
206 to the middle of the barnacle zone. The acclimation water temperatures were calculated by
207 averaging at least one year of water temperature data from the nearest water monitoring station.
208 Animals were acclimated to the conditions for at least a week before each respiration trial and re-
209 acclimated for at least one week between trials. They were starved for 48 hours prior to each
210 trial.

211

212 Table 1. Laboratory tidal cycles and abiotic conditions used for each population.

	Friday Harbor, WA	**Bodega Bay, CA**	**Southern California**
Low Tide 1		7:30am – 12:30 pm	
High Tide 1		12:30pm – 7:30pm	
Low Tide 2	7:30pm – 10:30pm	7:30pm-3:30am	7:30pm – 1:30am
High Tide 2	10:30pm – 7:30am	3:30am-7:30am	1:30am – 7:30 am
Lights on	03:30am – 7:30pm	04:45am – 07:00pm	
Water Temperature	10°C	12°C	18°C
Air Temperature		18-20 °C	

213

Respiration experiment

Full methods for the respiration protocol are reported in Ober et al. [38]. Briefly, about 30 minutes before the end of the "High Tide 2" phase of the laboratory tidal cycle (Table 1), barnacles were placed into individual aerial respiration chambers filled with filtered seawater. These were submerged in a temperature-controlled water bath at the acclimation water temperature. After 30 minutes, the water was siphoned out of the chambers and the water bath was heated or cooled until the chambers reached the experimental temperature. They were maintained at the experimental temperature for the remainder of the 5-hr low tide period. Oxygen concentrations in the chambers were recorded every 10-seconds with a fluorometric oxygen system with non-invasive sensor spots (Fibox 4 with Pst3-NAU spots, PreSens Precision Sensing, Regensburg, Germany). An empty chamber was included as a control. Afterwards, the barnacles were transferred to individual aquatic respiration chambers and submerged in a second water bath at the population's acclimation water temperature. Aquatic respiration was monitored for 6 hours as intertidal species can show elevated oxygen demand after emersion ["oxygen debt", 50].

While Ober et al. [38] used a fixed ramping rate of 10°C hr-1 for the FH population, this study used a fixed ramping period of 2.5 hrs. To facilitate comparisons among sites, we only used emersion data from the last 2.5 hours of each emersion trial, when all trials were at the experimental temperature. Additionally, in the present study we used 8 blocks of 4 barnacles from SC and BB, with each block used at two different temperatures, for a total of 8 barnacles per temperatures. The FH experiment used 9 barnacles per temperature, in blocks of 3.

Calculation of respiration rates

Slopes of change in oxygen concentration were calculated every five minutes for the last 2.5 hours of the emersion phase and the full six hours of the immersion phase. Slopes were only calculated for intervals with at least 10 data points. We divided the emersion observations by the control value before calculating the slope, in order to correct for the effect of pressure changes on the oxygen readings within the vials during the ramping phase. For aquatic data, we subtracted the slope of the control chamber from each experimental chamber to control for backgrounds rates of oxygen consumption within the seawater. If a control slope was missing for a five-minute aquatic interval, we substituted the average control slope for that trial. We used the five-minute slopes to calculate mean respiration rates for every 30 minutes of the last 2.5 hours of the emersion phase and for every hour of the immersion phase. For this we used 10% trimmed means to systematically exclude outliers. All calculations were completed using the Presens Oxygen Calculator (v 2.2.6) and R (v 4.2.2).

Statistical analysis

All statistical analyses were done in R 4.2.2, using the packages lme4 v. 3.1.160 [51], nlme v. 1.1.31 [52], car 3.1-1[53], and emmeans 1.8.3 [54]. Models were tested for departures from normality and homoscedasticity as described in [55]. In all models that included size as covariate, we used (Operculum Length)$^{1.8533}$, based on a previously reported allometric relationship [49]. The fixed effects were tested with type II likelihood ratio χ^2 tests, using the Anova function of car. We adjusted for multiple comparisons among sites using the Tukey method. We used the deltaMethod function of the car package to compare nonlinear parameter combinations.

To compare the intertidal and water DPMs, we used analysis of variance with autocorrelated errors in the gls function of nlme. We also compared the 75%ile of the intertidal temperatures using the rq function of the quantreg package v. 5.94 [56].

To compare thermal physiology thresholds among populations, we fit quadratic thermal performance curves in each medium and compared the location of T_{peak}. We first averaged across the hourly or half-hourly time points to calculate an average respiration rate per barnacle. We then estimated the thermal performance curves for each population in each medium as a parabola of the form: $\mu mol\ O_2 = ß_{1,P} + ß_{2,P}T + ß_{3,P}T^2 + ß_4 Op^{1.8533}$. Where P=source population, T=temperature, and Op=operculum length. From this we calculated T_{peak} for each population as $\frac{-ß_2}{2ß_3}$-. We selected this simple quadratic curve as curves with fewer parameters are recommended when there are a small number of study temperatures [15]. We included barnacle identity as a random factor to control for repeated measures on the same barnacle. Due to significant error heteroskedasticity, both models included extra error terms to allow for heterogeneous variances among temperature treatments (immersion) or temperatures and source populations (emersion).

We also looked for temperature thresholds by comparing the temporal pattern of oxygen consumption in each medium. For example, a decreasing emersion respiration rate over time could suggest physiological impairment, while the same pattern during immersion would be consistent with an oxygen debt [50]. For this analysis, we fit separate mixed-model ANCOVAs for each medium. These models treated temperature (T) as a categorical variable and also included source population (P) and time point (H) as categorical factors and Operculum Length (Op) as a covariate. They were of the form: $\mu mol\ O_2 = ß_1 + ß_2P + ß_3H + ß_4T + ß_5PH + ß_6PT + ß_7HT + ß_8PHT + ß_9Op^{1.8533}$. Barnacle identity was included as a random factor to control for

280 repeated measurements on the same barnacle. Due to significant error heteroskedasticity, both
281 models included an extra error term to allow heterogeneous variances among trial dates. One
282 data point for an FH barnacle at 38°C at the 30-minute point was excluded from the emersion
283 data set, as it was 5-fold larger than any other data point. Polynomial contrasts were used to
284 identify respiration patterns over time within each combination of source population and
285 experimental temperature.

286 Vulnerability to warming

287 To estimate each population's vulnerability to warming temperatures, we first calculated
288 the cost of a 30-emersion at each temperature for each phase of the trial, using the estimated
289 marginal means (EMM) from the analyses above. For the cost during emersion, we multiplied
290 the 5-minute EMM values from the emersion TPC by 6 to scale up to 30 minutes. For the cost
291 during immersion, we subtracted off a basal rate of oxygen consumption from the immersion
292 TPC EMMs, using the EMM for hour 6 of each trial, and then multiplied by 72 to get the full
293 oxygen debt for the 6-hr immersion trial. We divided this value by 5 to adjust it from the 2.5-
294 hour emersion exposure of the trial to a 30-emersion exposure. Finally, we summed the
295 emersion and immersion values to get the total energetic cost of a 30-minute emersion at each
296 temperature.

297 We used these values to calculate vulnerability in two ways: as the number of days spent
298 above T_{peak} and as the total costs of emersion over the year. In the first case, we fit a new TPC
299 parabola for each population from the total cost values and calculated T_{peak} as described above.
300 In the second case, because costs increase with temperature even though TPC curves decline at
301 high temperatures (Fig 1), we used the regression approach of Ober et al. [38] to calculate an
302 exponentially increasing total cost function based on the metabolic theory of ecology equation

303 [21,57], excluding temperatures above the peak of the total cost curve (or below the minimum
304 for SC).

305 Results

306 Field temperatures

307 There was clear pattern of declining water temperatures with increasing latitude, but no
308 such pattern for intertidal temperatures (Fig 3). Both intertidal ($F_{2,1093} = 21.8$, $p<0.0001$) and
309 water ($F_{2,1093} = 38.02$, $p<0.0001$) DPMs showed significant differences among sites, driven
310 mainly by the southernmost SC site. Compared to BB and FH, the mean intertidal DPM at the
311 SC site warmer 7-10°C warmer and the mean water DPM were more than 6°C warmer ($p <$
312 0.01). The northernmost FH site had 3°C cooler water DPMs and 1.5°C warmer intertidal DPMs
313 than the BB site, but these differences were not significant ($p >0.05$). However, a comparison of
314 the 75th percentile of the intertidal DPMs, using quantile regression, revealed statistically
315 significant differences among all pairs of populations ($p<0.004$ for each comparison), with the
316 northernmost (FH) site being 4.5°C cooler than SC and 1.9°C warmer than BB.
317
318 **Figure 3. Box plot of daily 97.9%ile of intertidal data logger and water temperatures at**
319 **each site over one year**. The top and bottom of the box indicate the 25th and 75th percentiles.
320 The notched line is the median. The notch height estimates 95% CIs around the median.
321

322 Thermal performance curves

323 When respiration rates were pooled over timepoints, both the immersion and emersion
324 analyses revealed a statistically significant quadratic term, indicating that parabolas fit the

respiration data better than linear regression (Table 2A). There were also significant interactions between population and both the linear and quadratic temperature terms, indicating differences in the shape or position of the parabolas among the three populations (Table 2A, Fig 4). The fitted parabolas (Table 2B) for emersion for the two most northern populations were concave, with T_{peak} estimated at 27.5°C (23.8-31.2 95%CI) for FH and 24.9°C (19.2-30.5 95%CI) for BB (Fig 4a and 4c). In contrast, the parabola for SC (Table 2B) was convex (Fig 4e), with a minimum respiration rate at 20.0°C (14.4-25.6 95%CI). The shallow, convex shape of the SC curve suggests that we did not measure temperatures high enough to capture T_{peak} for this population.

A similar pattern was seen in the immersion curves (Table 2B). The two most northern populations were concave, with T_{peak} estimated at 23.6°C (22.3-25.0 95%CI) for FH and 19.4 °C (13.2-25.5 95%CI) for BB (Fig 4b and 4d). But the southern site (SC) again showed a convex pattern (Fig 4f), with a minimum respiration rate at 20.9°C (4.9 – 36.9 %CI). Multiple comparisons tests revealed a significant difference in the location between the emersion peaks for FH and SC (p=0.028), but no other differences were significant (p>0.05).

Table 2. Model results for average oxygen consumption, treating temperature as a continuous variable. Analysis of deviance statistics for each medium (A) and parameter estimates (+se) for the line of best fit from the model for each population (B).

A)	**Emersion**			**Immersion**		
Term	χ^2	df	p	χ^2	df	p
Population	32.5011	2	<0.0001	3.2237	2	0.1995
Temperature	2.5823	1	0.1081	13.0248	1	0.0003
Temperature^2	0.8269	1	0.3632	16.6997	1	< 0.0001

Size	5.1147	1	0.0237	12.8529	1	0.0003
Pop x Temp	26.224	2	<0.0001	13.5512	2	0.0011
Pop x Temp^2	32.5011	2	<0.0001	16.1523	2	0.0003

B)	**Bodega Bay**	**Friday Harbor**	**Southern California**
Emersion			
Intercept	-0.03280 (0.02094)	-0.09348 (0.0235)	0.00059 (0.01494)
Temperature	0.00122 (0.00056)	0.00353 (0.00185)	0.00935 (0.00201)
Temperature^2	-0.00142 (0.00101)	-0.00007 (0.00004)	-0.00017 (0.00005)
Operculum Length	0.00004 (0.00002)	0.00004 (0.00002)	0.00004 (0.00002)
Immersion			
Intercept	-0.01169 (0.01698)	-0.05631 (0.01585)	-0.00053 (0.01652)
Temperature	0.0022 (0.00138)	0.00546 (0.00117)	-0.00071 (0.00132)
Temperature^2	-0.00006 (0.00003)	-0.00012 (0.00002)	0.00002 (0.00003)
Operculum Length	0.00131 (0.00038)	0.00131 (0.00038)	0.00131 (0.00038)

Figure 4. Oxygen consumption by temperature for each population during emersion (A-C) and Immersion (D-F). Parabolas represent the predicted respiration rates from the mixed model, calculated at the mean overall size of the experiment (5.05 mm operculum length). Dashed lines estimate T_{peak} values. The individual points represent mean respiration rates for individual barnacles, with the darkness of the fill indicating size.

352 # Temporal patterns of respiration by medium

353 ## Emersion

354 The emersion respiration rates ranged from 0.0018 to 0.057 µmol/5min, depending on the
355 source population, temperature, and time point (Fig 5). All terms in the mixed model ANCOVA
356 for emersion were statistically significant, including the three-way interaction between source
357 population, time, and treatment temperature (Table 3). There was also a significant main effect
358 of population, with the highest overall respiration rates at FH at most temperatures. Most
359 combinations of source population and temperature showed little variation across timepoints,
360 with two exceptions. Within the southernmost (SC) population, all but the two lowest and one
361 highest temperature showed a significantly increasing linear trend in respiration rates over the
362 2.5 hr. period. Above 20 °C, both BB and FH showed linearly decreasing trends over time.

363

364 **Figure 5. Average emersion oxygen consumption by temperature and time point for each**
365 **population.** Gray lines represent data for individual barnacles, darkness reflects size. Estimated
366 marginal means (±95CI), for a barnacle of 5.05 mm operculum length, are shown in red. Letters
367 indicate significant polynomial contrasts ($p<0.05$, L=Linear, Q=Quadratic)

368

369 **Table 3. Analysis of deviance for respiration by population and timepoint during emersion**
370 **and immersion.**

	Emersion			**Immersion**		
Term	χ^2	df	p	χ^2	df	p
Population	36.6454	2	<0.0001	4.8558	2	0.0882
Time	7.7978	4	0.0993	76.7112	5	<0.0001

Temperature	204.9101	6	<0.0001	288.4884	6	<0.0001
Size	4.5776	1	0.0324	8.8019	1	0.0030
Pop x Time	71.1303	8	<0.0001	10.7962	10	0.3736
Pop x Temp	237.3474	12	<0.0001	349.9856	12	<0.0001
Temp x Time	235.9039	24	<0.0001	97.2488	30	0.0000
Pop x Time x Temp	294.976	48	<0.0001	128.1517	60	0.0000

Immersion

Average immersion respiration rates ranged from 0.0071 to 0.0431 µmol/5min, depending on the source population, temperature, and time point (Fig 6). The mixed model analysis revealed a significant overall effect of emersion temperature on immersion respiration, as well as significant differences among populations in the form of interactions between population and temperature and between population, temperature, and hour (Table 3). There were three distinct temporal patterns among the temperatures (Fig 6). At the coolest temperatures we frequently detected a significant quadratic trend, where immersion respiration rates tended to be lowest in the first hour post emersion, peak in the second or third hour, and then decline. This pattern occurred at temperatures between 10-20°C at the central BB site, between 10-25°C at the northern FH site and at temperatures up to 30°C at the southern SC site, although the quadratic trend was not always statistically significant (Fig 6). Above these temperatures, the pattern shifted to a linear negative trend, indicating higher respirations rates in the first 1-2 hours post emersion. This occurred at 25 and 35°C for BB, 30 and 35°C for FH and 35°C for SC. The transition between the first two patterns for FH and BB corresponds with the estimated emersion T_{peak} values for those populations. Finally, at 35 and 38°C for BB and at 38°C for the other two sites, respiration was initially depressed and then increased over time.

389

390 **Figure 6. Aquatic oxygen consumption by temperature and hour for each population.**
391 Estimated marginal means (±95CI), for a barnacle of 5.05 mm operculum length, are shown in
392 red. Gray lines are data for individual barnacles, with the darkness of the line indicating size.
393 Letters indicate significant polynomial contrasts ($p<0.05$, L=Linear, Q=Quadratic). Colored bars
394 indicate qualitative assignment of respiration rates pattern to non-stressful (Blue), increased
395 energy demand (Orange), and physiological damage (Yellow).

396

397 # Total cost of emersion and vulnerability to warming

398 The estimated total cost of a 30-minute emersion ranged from -0.07µmol for BB
399 barnacles at 38°C to 0.66µmol for FH barnacles at 25°C (Fig 7A). On average, immersion
400 respiration accounted for 18% of the total cost of exposure, but this ranged from 0 to nearly 50%,
401 depending on the temperature and population. As before, the fitted parabolas for the total cost for
402 the two most northern populations were concave (Table 4), with T_{peak} estimated at 25.1°C
403 (25.12-25.12%CI) for FH and 21.3 (21.3-21.3%CI) for BB (Fig 7); while the parabola for SC
404 was convex, with a minimum cost at 20.5°C (20.5-20.5 95%CI, Table 4). The MTE-based cost
405 curves showed increasing costs with latitude (Fig 7A, Table 4).

406 When we compared the number of days above T_{peak} for each site, substituting 38°C for
407 the SC T_{peak} (Fig 7C), we found BB to be most vulnerable, with 149 days over T_{peak}, followed by
408 FH (93 days) and SC (4 days). The total annual costs (Fig 7B) followed the pattern of the MTE
409 costs curves (Fig 7A), with FH showing the highest energy costs and SC the lowest.

410

411 **Figure 7. Total cost of a 30-minute emersion exposure by temperature (A), total annual**

412 **cost for each population (B), and number of days over T_{Peak} (C).**

413

414 **Table 4. Parameter values (±SE) for the total costs equations fitted for each population.**

	Friday Harbor	Bodega Bay	Southern California
Parabola TPC			
Intercept	-1.04 (1.63E-15)	-0.285 (1.63E-15)	0.257 (1.63E-15)
Temperature	0.135 (1.49E-16)	0.0529 (1.49E-16)	-0.0187 (1.49E-16)
Temperature^2	-0.00268 (3.04E-18)	-0.00124 (3.04E-18)	0.000457 (3.04E-18)
Exponential TPC			
-E	48.43 (11.32)	22.53 (17.74)	17.77 (8.99)
$\ln(R_o)$	-14434.01 (3287.7)	-6961.4 (5111.17)	-6042.32 (2721.12)

415

416 # Discussion

417 Identifying the species and populations most vulnerable to climate change is a critical

418 priority for ecologists. Studies of intraspecific biogeographic variation in thermal physiology,

419 particularly of species that do not experience strong latitudinal clines in thermal conditions, are

420 needed to test and further develop models of geographic-scale thermal physiology. Overall, our

421 results suggest that, consistent with the Climate Extremes and Climate Variability hypotheses,

422 the extreme temperatures experienced during emersion are driving the thermal physiology of

423 these three populations of *Balanus glandula*. We found that the peaks (T_{peak}) of the respiration

424 curves in all three populations were well above the range of aquatic temperatures at each site and

425 better matched to differences in the emersion thermal regimes among sites. These conclusions
426 are tempered by the small thermal differences between our two northernmost sites which limited
427 the statistical significance of some comparisons. We also found different patterns of
428 vulnerability to warming temperatures, depending on the metric of vulnerability used. The most
429 vulnerable site according to the cost approach was the northernmost site, while it was the central
430 site according to the threshold approach. This discrepancy arises from the large differences we
431 observed in energy demand among our three populations, which may reflect local adaptation to
432 variation in nearshore ocean productivity and food supply.

433 Intertidal organisms experience two distinct thermal regimes during emersion and
434 immersion and it unclear which drives thermal physiology, particularly at warmer temperatures
435 [24,26,33,34]. Three lines of evidence in this study suggest that the extreme temperatures
436 experienced during low tide conditions drive the thermal physiology of *B. glandula*. First, the
437 identified T_{peak} of each population is well above its site's aquatic DPMs. A population's T_{peak}
438 should exceed its average DPM to minimize the amount of time spent at stressful temperatures
439 [58]. But, these T_{peak} values exceed even the maximum water temperatures observed at each site.
440 Second, the ordering of the thermal peaks of the northern FH and central BB sites match the
441 ordering of emersion DPMs rather than immersion DPMs. The emersion temperature
442 differences at these two sites were small and sensitive to the temperature metric used (mean vs.
443 75%ile). However, similarly small temperatures differences can greatly influence intertidal
444 community composition and population dynamics [59]. We found similar results in a separate
445 study that measured aquatic respiration rates in barnacles acclimated to different immersion
446 temperatures (Ober et al. *in prep*): aquatic respiration rates in all three populations peaked at

447 water temperatures well over local maxima and the northern FH population again had a warmer
448 T_{peak} than BB.

449 It also appears that the T_{peak} values for the southernmost (SC) population are greater than
450 the highest temperature we tested (38°C), placing them well above the T_{peak} values for BB and
451 FH. This is surprising, given that a 40°C emersion is lethal for FH barnacles [38]. However, it
452 is consistent with the warmer overall temperatures at this site and with previously identified
453 genetic differences among populations [37,42]. Unfortunately, because both the aquatic and
454 intertidal thermal environments at the southern SC site are so much warmer than the two other
455 sites, comparisons with SC do not inform the question of whether aquatic or terrestrial
456 environments are the main driver of these physiological differences.

457 The third line of evidence that emersion conditions drive warm temperature
458 physiology is in the temporal patterns of oxygen use during the immersion phase of the
459 experiment. We detected three distinct temporal patterns of respiration during immersion.
460 Consistent with FH having a more warm-adapted physiology than BB, the transition between
461 each pattern occurred at a warmer temperature for FH than for BB. At the coolest temperatures,
462 barnacles exhibited parabolic patterns with initially low respiration rates that increased in the
463 second or third hour of immersion and then declined. This pattern indicates a non-stressful
464 emersion temperature. We hypothesize that barnacles initially reduced respiration upon
465 immersion because they had access to sufficient oxygen during emersion and were not
466 experiencing high energy demand. Video observations of the FH population [38] indicate that *B.*
467 *glandula* are frequently closed in the first few hours of immersion at these cooler temperatures.
468 Similar patterns of low post-emersion oxygen demand have been reported in other high shore
469 barnacle species [60]. The concentration of oxygen in air is roughly 20-fold higher than in

470 seawater, so oxygen may be more accessible during emersion at moderate temperatures then
471 during immersion [61]. By staying closed barnacles may also reduce to vulnerability predation
472 during immersion [62].

473 At warmer temperatures, barnacles began immersion with higher initial respiration rates
474 that declined gradually over the 6-hr immersion period. These barnacles also often showed a
475 decline in emersion respiration over time. The high initial immersion activity was also observed
476 in video data recorded from FH barnacles [38] and suggests that high energy demand during
477 emersion created an immediate need for respiration upon resubmersion. This is typically
478 described as an oxygen debt in the literature [50,63]. Finally, at the warmest temperatures,
479 respiration was depressed and remained low for several hours. This third pattern suggests
480 physiological impairment. At these temperatures the barnacles often appeared in a heat coma
481 during immersion with cirri extended but not moving.

482 The second goal of this study was to assess each population's vulnerability to warming
483 temperatures under climate change. Our assessment of vulnerability varied with the metric of
484 vulnerability. When we calculated the total annual costs of exposure to intertidal DPM
485 temperatures, the northernmost FH population had the greatest total energy cost among the three
486 sites. However, when we calculated the number of days above T_{peak}, the central BB site
487 appeared most vulnerable. We were unable to identify any published studies that compared
488 these two metrics of vulnerability, so it is unclear how common our result is. But it suggests that
489 estimates of vulnerability to warming are highly sensitive to the metric used.

490 One possible explanation for the greater energetic costs at FH may be differences in food
491 availability at each site. *Balanus glandula*'s exact diet is unknown [64], but they likely consume
492 a range of phytoplankton and zooplankton, as adults can thrive on either in the laboratory

493 [49,65,66]. There is a strong latitudinal gradient in primary productivity throughout this region
494 of the northeastern Pacific, with coastal Washington State and British Columbia exhibiting 5-
495 fold greater chlorophyll concentrations than California [67,68], along with higher zooplankton
496 concentrations [67]. This gradient is attributed to greater terrestrial nutrient supply at higher
497 latitudes, particularly in the Salish Sea region [68], which includes the FH field site. A greater
498 food supply could select for greater energy use in the two higher latitude populations, while the
499 SC (southernmost) barnacles may be adapted to succeed in a lower resource environment. This
500 is an alternate explanation for previously described genetic cline in *B. glandula* [36,42].

501 Conclusion

502 The results presented herein provide strong evidence that thermal conditions experienced
503 during emersion do influence the thermal physiology of the intertidal barnacle *Balanus glandula*.
504 However, more empirical studies are needed to fully test the Climate Extremes and Climate
505 Variability Hypotheses in intertidal species. The possibility that *B. glandula* populations are
506 locally adapted or acclimated to both thermal regimes and food supplies complicates predictions
507 of their response to warming temperatures. While its well-established that food supply can limit
508 many ectotherms' tolerance of thermal stress [e.g., 69,70], few models of climate change
509 responses have considered both warming temperatures and changes in food supply at the same
510 time (but see [71]). While its higher overall energy demand suggests that the FH population is
511 the most vulnerable to warming temperatures, phytoplankton productivity is also predicted to
512 increase in this region under climate change [72]. Thus, in this case, the threshold approach may
513 provide a better estimate of vulnerability to future warming for *Balanus glandula*.

References

1. Gaston KJ, Chown SL, Calosi P, Bernardo J, Bilton DT, Clarke A, et al. Macrophysiology: a conceptual reunification. Am Nat. 2009;174: 595–612. doi:10.1086/605982

2. Bennett S, Duarte CM, Marbà N, Wernberg T. Integrating within-species variation in thermal physiology into climate change ecology. Philos Trans R Soc B Biol Sci. 2019;374: 20180550. doi:10.1098/rstb.2018.0550

3. Helmuth B, Harley CDG, Halpin PN, O'Donnell M, Hofmann GE, Blanchette CA. Climate change and latitudinal patterns of intertidal thermal stress. Sci Wash C. 2002;298: 1015–1017.

4. Deutsch CA, Tewksbury JJ, Huey RB, Sheldon KS, Ghalambor CK, Haak DC, et al. Impacts of climate warming on terrestrial ectotherms across latitude. Proc Natl Acad Sci. 2008;105: 6668–6672.

5. Gilman SE, Wethey DS, Helmuth B. Variation in the sensitivity of organismal body temperature to climate change over local and geographic scales. Proc Natl Acad Sci U S A. 2006;103: 9560–9565. doi:10.1073/pnas.0510992103

6. Gaitan-Espitia JD, Bacigalupe LD, Opitz T, Lagos NA, Osores S, Lardies MA. Exploring physiological plasticity and local thermal adaptation in an intertidal crab along a latitudinal cline. J Therm Biol. 2017;68: 14–20. doi:10.1016/j.jtherbio.2017.02.011

7. Gunderson AR, Dillon ME, Stillman JH. Estimating the benefits of plasticity in ectotherm heat tolerance under natural thermal variability. Funct Ecol. 2017;31: 1529–1539. doi:10.1111/1365-2435.12874

8. Porter WP, Gates DM. Thermodynamic equilibria of animals with environment. Ecol Monogr. 1969;39: 245–270.

9. Fey SB, Vasseur DA, Alujevic K, Kroeker KJ, Logan ML, O'Connor M, et al. Opportunities for behavioral rescue under rapid environmental change. Glob Change Biol. 2019;25: 3110–3120. doi:10.1111/gcb.14712

10. Hayford HA, Gilman SE, Carrington E. Tidal cues reduce thermal risk of climate change in a foraging marine snail. Clim Change Ecol. 2021;1: 100003. doi:10.1016/j.ecochg.2021.100003

11. Sunday J, Bennett JM, Calosi P, Clusella-Trullas S, Gravel S, Hargreaves AL, et al. Thermal tolerance patterns across latitude and elevation. Philos Trans R Soc B Biol Sci. 2019;374: 20190036. doi:10.1098/rstb.2019.0036

12. Buckley LB, Huey RB, Kingsolver JG. Asymmetry of thermal sensitivity and the thermal risk of climate change. Glob Ecol Biogeogr. 2022;31: 2231–2244. doi:10.1111/geb.13570

548 13. Sunday JM, Bates AE, Dulvy NK. Global analysis of thermal tolerance and latitude in
549 ectotherms. Proc R Soc B Biol Sci. 2010;278: 1823–1830. doi:10.1098/rspb.2010.1295

550 14. Tagliarolo M, McQuaid CD. Sub-lethal and sub-specific temperature effects are better
551 predictors of mussel distribution than thermal tolerance. Mar Ecol Prog Ser. 2015;535:
552 145–159. doi:10.3354/meps11434

553 15. Low-Décarie E, Boatman TG, Bennett N, Passfield W, Gavalás-Olea A, Siegel P, et al.
554 Predictions of response to temperature are contingent on model choice and data quality.
555 Ecol Evol. 2017;7: 10467–10481. doi:10.1002/ece3.3576

556 16. Fly EK, Monaco CJ, Pincebourde S, Tullis A. The influence of intertidal location and
557 temperature on the metabolic cost of emersion in *Pisaster ochraceus*. J Exp Mar Biol Ecol.
558 2012;422: 20–28. doi:10.1016/j.jembe.2012.04.007

559 17. Kooijman SALM. Dynamic energy budget theory for metabolic organisation. Cambridge;
560 New York: Cambridge University Press; 2010.

561 18. Lemoine NP, Burkepile DE. Temperature-induced mismatches between consumption and
562 metabolism reduce consumer fitness. Ecology. 2012;93: 2483–2489.

563 19. Mislan KAS, Helmuth B, Wethey DS. Geographical variation in climatic sensitivity of
564 intertidal mussel zonation. Glob Ecol Biogeogr. 2014;23: 744–756. doi:10.1111/geb.12160

565 20. Monaco CJ, Wethey DS, Helmuth B. A dynamic energy budget (DEB) model for the
566 keystone predator *Pisaster ochraceus*. Plos One. 2014;9: e104658.
567 doi:10.1371/journal.pone.0104658

568 21. Dell AI, Pawar S, Savage VM. Systematic variation in the temperature dependence of
569 physiological and ecological traits. Proc Natl Acad Sci. 2011;108: 10591–10596.

570 22. McMahon RF. Thermal tolerance, evaporative water loss, air-water oxygen consumption and
571 zonation of intertidal prosobranchs: a new synthesis. Hydrobiologia. 1990;193: 241–260.
572 doi:10.1007/BF00028081

573 23. Sokolova IM, Portner HO. Physiological adaptations to high intertidal life involve improved
574 water conservation abilities and metabolic rate depression in *Littorina saxatilis*. Mar Ecol
575 Prog Ser. 2001;224: 171–186. doi:10.3354/meps224171

576 24. Sanford E. Water temperature, predation, and the neglected role of physiological rate effects
577 in rocky intertidal communities. Integr Comp Biol. 2002;42: 881–891.
578 doi:10.1093/icb/42.4.881

579 25. Iles AC. Toward predicting community-level effects of climate: relative temperature scaling
580 of metabolic and ingestion rates. Ecology. 2014;95: 2657–2668.

581 26. Somero GN. Thermal physiology and vertical zonation of intertidal animals: Optima, limits,
582 and costs of living. Integr Comp Biol. 2002;42: 780–789. doi:10.1093/icb/42.4.780

27. Sunday J, Bennett JM, Calosi P, Clusella-Trullas S, Gravel S, Hargreaves AL, et al. Thermal tolerance patterns across latitude and elevation. Philos Trans R Soc B Biol Sci. 2019;374: 20190036. doi:10.1098/rstb.2019.0036

28. Byun D-S, Hart DE, Kim S, Ha J. Classification of monthly tidal envelopes in mixed tide regimes. Sci Rep. 2023;13: 4786. doi:10.1038/s41598-023-31657-x

29. Denny MW. Tides. 1st ed. In: Denny MW, Gaines SD, editors. Encyclopedia of Tides and Rocky Shores. 1st ed. University of California Press; 2007. pp. 588–595. Available: http://www.jstor.org/stable/10.1525/j.ctt1pnt4d.24

30. Helmuth B, Broitman BR, Blanchette CA, Gilman S, Halpin P, Harley CDG, et al. Mosaic patterns of thermal stress in the rocky intertidal zone: Implications for climate change. Ecol Monogr. 2006;76: 461–479. doi:10.1890/0012-9615(2006)076[0461:MPOTSI]2.0.CO;2

31. Gleason LU, Burton RS. Phenotypic evidence for local adaptation to heat stress in the marine snail *Chlorostoma* (formerly *Tegula*) *funebralis*. J Exp Mar Biol Ecol. 2013;448: 360–366. doi:10.1016/j.jembe.2013.08.008

32. Sagarin RD, Somero GN. Complex patterns of expression of heat-shock protein 70 across the southern biogeographical ranges of the intertidal *mussel Mytilus californianus* and snail *Nucella ostrina*. J Biogeogr. 2006;33: 622–630. doi:10.1111/j.1365-2699.2005.01403.x

33. Rao KP. Rate of water propulsion in *Mytilus californianus* as a function of latitude. Biol Bull. 1953;104: 171–181. doi:10.2307/1538791

34. Logan CA, Kost LE, Somero GN. Latitudinal differences in *Mytilus californianus* thermal physiology. Mar Ecol Prog Ser. 2012;450: 93–105. doi:10.3354/meps09491

35. Morris RH, Abbott DP, Haderlie EC. Intertidal Invertebrates of California. 1st ed. Stanford, Calif: Stanford University Press; 1980.

36. Sotka EE, Wares JP, Barth JA, Grosberg RK, Palumbi SR. Strong genetic clines and geographical variation in gene flow in the rocky intertidal barnacle *Balanus glandula*. Mol Ecol. 2004;13: 2143–2156.

37. Wares JP, Skoczen KM. Maintenance of a genetic cline in the barnacle *Balanus glandula*. Biol Bull. 2019;236: 199–206. doi:10.1086/703516

38. Ober GT, Rognstad RL, Gilman SE. The cost of emersion for the barnacle *Balanus glandula*. Mar Ecol Prog Ser. 2019;627: 95–107. doi:10.3354/meps13058

39. Geller J, Sotka EE, Kado R, Palumbi SR, Schwindt E. Sources of invasions of a northeastern Pacific acorn barnacle, *Balanus glandula*, in Japan and Argentina. Mar Ecol Prog Ser. 2008;358: 211–218. doi:10.3354/meps07466

40. Simon-Blecher N, Granevitze Z, Achituv Y. *Balanus glandula*: from North-West America to the west coast of South Africa. Afr J Mar Sci. 2008;30: 85–92. doi:10.2989/ajms.2008.30.1.8.458

41. Helmuth B, Choi F, Matzelle A, Torossian JL, Morello SL, Mislan K a. S, et al. Long-term, high frequency in situ measurements of intertidal mussel bed temperatures using biomimetic sensors. Sci Data. 2016;3: 160087. doi:10.1038/sdata.2016.87

42. Wares JP, Strand AE, Sotka EE, Bernardi G. Diversity, divergence and density: How habitat and hybrid zone dynamics maintain a genomic cline in an intertidal barnacle. J Biogeogr. 2021;48: 2174–2185. doi:10.1111/jbi.14142

43. National Oceanic and Atmospheric Administration. Station Home Page - NOAA Tides & Currents. In: Station Home Page: 9449880 Friday Harbor, WA [Internet]. [cited 15 Feb 2024]. Available: https://tidesandcurrents.noaa.gov/stationhome.html?id=9449880

44. Quinn JF, Wolin CL, Judge ML. An experimental analysis of patch size, habitat subdivision, and extinction in a marine intertidal snail. Conserv Biol. 1989;3: 242–251. doi:10.1111/j.1523-1739.1989.tb00084.x

45. Bodega Ocean Observing Node. [cited 18 Feb 2024]. Available: https://boon.ucdavis.edu/

46. ERDDAP - SCCOOS Automated Shore Station - Data Access Form. [cited 18 Feb 2024]. Available: https://erddap.sccoos.org/erddap/tabledap/autoss.html

47. Wethey DS. Biogeography, competition, and microclimate: The barnacle *Chthamalus fragilis* in New England. Integr Comp Biol. 2002;42: 872–880. doi:10.1093/icb/42.4.872

48. Helmuth BST, Hofmann GE. Microhabitats, thermal heterogeneity, and patterns of physiological stress in the rocky intertidal zone. Biol Bull. 2001;201: 374–384. doi:10.2307/1543615

49. Gilman SE, Chen S, Wong JWH. Oxygen consumption in relation to body size, wave exposure, and cirral beat behavior in the barnacle *Balanus glandula*. J Crustac Biol. 2013;33: 317–322.

50. Ellington WR. The recovery from anaerobic metabolism in invertebrates. J Exp Zool. 1983;228: 431–444. doi:10.1002/jez.1402280305

51. Bates D, Maechler M, Bolker B, Walker S. Fitting Linear Mixed-Effects Models Using lme4. J Stat Softw. 2015;67: 1–48. doi:10.18637/jss.v067.i01.

52. Pinheiro J, Bates D, Team RC. _nlme: Linear and Nonlinear Mixed Effects Models_. 2022. Available: https://CRAN.R-project.org/package=nlme

53. Fox J, Weisberg S. An R Companion to Applied Regression. Thousand Oaks CA: Sage; 2019. Available: https://socialsciences.mcmaster.ca/jfox/Books/Companion/

54. Lenth RV. _emmeans: Estimated Marginal Means, aka Least-Squares Means_. R package version 1.8.3. 2022. Available: https://CRAN.R-project.org/package=emmeans

55. Zuur AF, Ieno EN, Smith GM. Analysing ecological data. New York ; London: Springer; 2007.

56. Koenker R. _quantreg: Quantile Regression_. R package version 5.94. 2022. Available: https://CRAN.R-project.org/package=quantreg

57. Brown JH, Gillooly JF, Allen AP, Savage VM, West GB. Toward a metabolic theory of ecology. Ecology. 2004;85: 1771–1789.

58. Martin TL, Huey RB. Why "suboptimal" Is optimal: Jensen's Inequality and ectotherm thermal preferences. Am Nat. 2008;171: E102–E118. doi:10.1086/527502

59. Harley CDG. Climate change, keystone predation, and biodiversity loss. Science. 2011;334: 1124–1127. doi:10.1126/science.1210199

60. Davenport J, Irwin S. Hypoxic life of intertidal acorn barnacles. Mar Biol. 2003;143: 555–563. doi:10.1007/s00227-003-1057-0

61. Hughes JS, Otto SP. Ecology and the evolution of biphasic life cycles. Am Nat. 1999;154: 306–320. doi:10.1086/303241

62. Horn KM, Fournet MEH, Liautaud KA, Morton LN, Cyr AM, Handley AL, et al. Effects of intertidal position on metabolism and behavior in the acorn barnacle, *Balanus glandula*. Integr Org Biol. 2021;3: obab010. doi:10.1093/iob/obab010

63. McGaw LJ, Clifford AM, Goss GG. Physiological responses of the intertidal starfish *Pisaster ochraceus*, (Brandt, 1835) to emersion at different temperatures. J Exp Mar Biol Ecol. 2015;468: 83–90. doi:10.1016/j.jembe.2015.03.019

64. Sanford E, Menge BA. Spatial and temporal variation in barnacle growth in a coastal upwelling system. Mar Ecol Prog Ser. 2001;209: 143–157. doi:10.3354/meps209143

65. Hines AH. Reproduction in three species of intertidal barnacles from central California. Biol Bull. 1978;154: 262–281.

66. Geierman C, Emlet R. Feeding behavior, cirral fan anatomy, Reynolds numbers, and leakiness of *Balanus glandula*, from post-metamorphic juvenile to the adult. J Exp Mar Biol Ecol. 2009;379: 68–76. doi:10.1016/j.jembe.2009.08.003

67. Ware D, Thomson R. Bottom-up ecosystem trophic dynamics determine fish production in the northeast Pacific. Science. 2005;308: 1280–1284. doi:10.1126/science.1109049

68. Hickey B, Banas N. Why is the northern end of the California Current System so productive? Oceanography. 2008;21: 90–107. doi:10.5670/oceanog.2008.07

69. Gilman SE. Life at the edge: an experimental study of a poleward range boundary. Oecologia. 2006;148: 270–279. doi:10.1007/s00442-006-0372-9

70. Schneider KR, Van Thiel LE, Helmuth B. Interactive effects of food availability and aerial body temperature on the survival of two intertidal *Mytilus* species. J Therm Biol. 2010;35: 161–166. doi:10.1016/j.jtherbio.2010.02.003

71. Huey RB, Kingsolver JG. Climate warming, resource availability, and the metabolic meltdown of ectotherms. Am Nat. 2019;194: E140–E150. doi:10.1086/705679

72. Khangaonkar T, Nugraha A, Xu W, Balaguru K. Salish Sea response to global climate change, sea level rise, and future nutrient loads. J Geophys Res Oceans. 2019;124: 3876–3904. doi:10.1029/2018JC014670

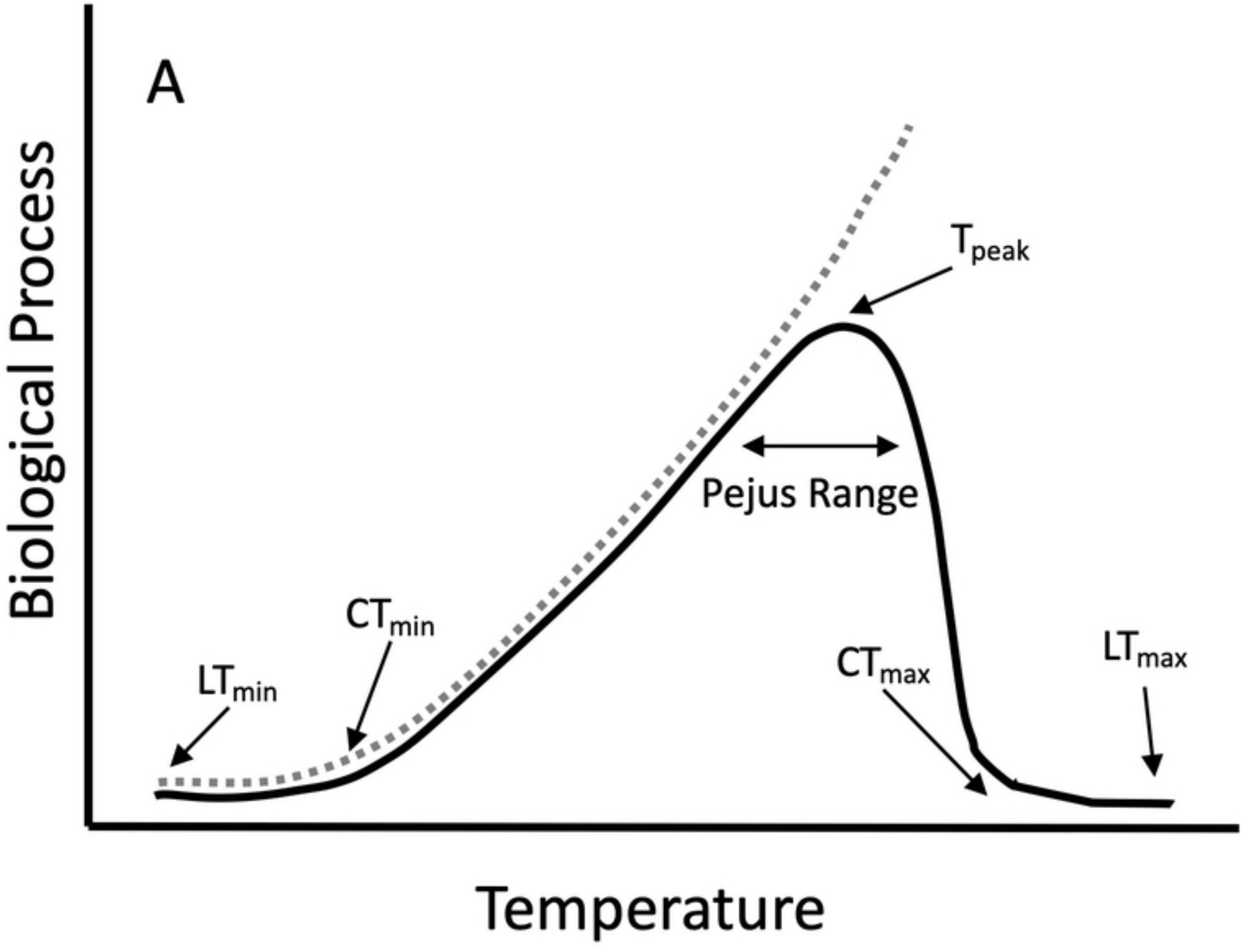
A
Biological Process
Temperature
T_{peak}
Pejus Range
CT_{min}
LT_{min}
CT_{max}
LT_{max}

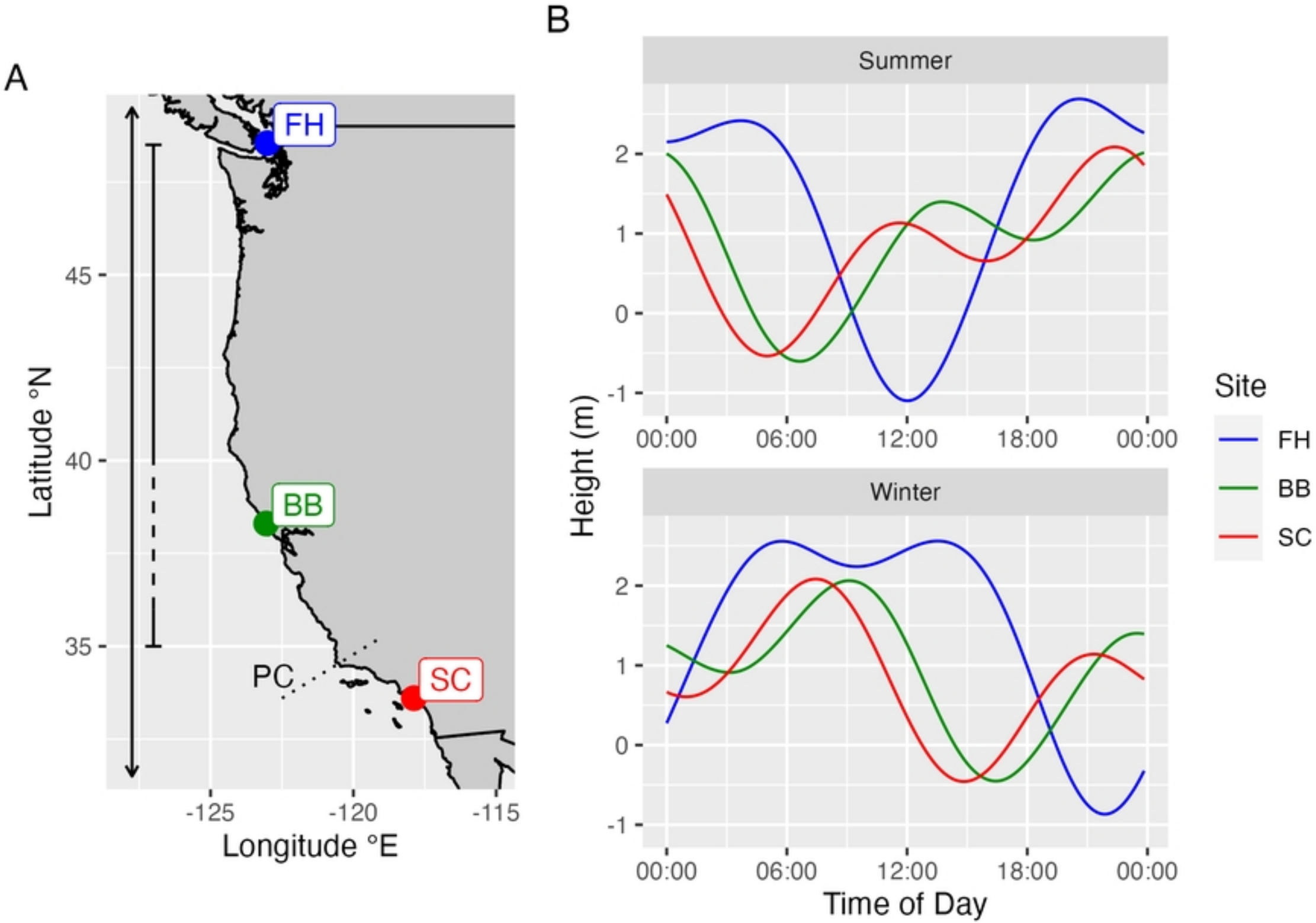
A
FH
BB
SC
PC
45
40
35
Latitude °N
-125
-120
-115
Longitude °E
B
Summer
Winter
Height (m)
2
1
0
-1
00:00
06:00
12:00
18:00
00:00
Time of Day
Site
FH
BB
SC

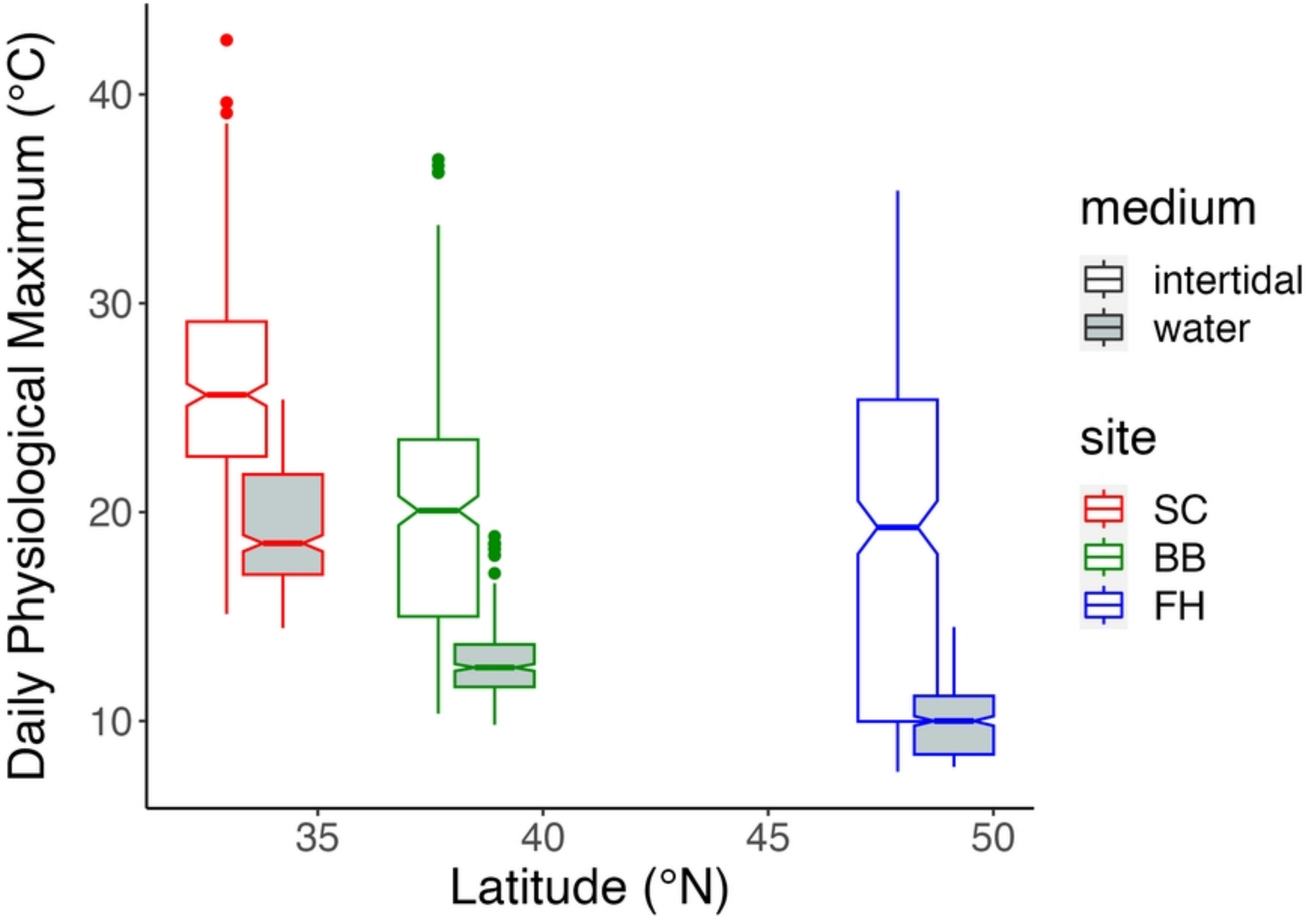
Daily Physiological Maximum (°C)
40
30
20
10
35
40
45
50
Latitude (°N)
medium
intertidal
water
site
SC
BB
FH

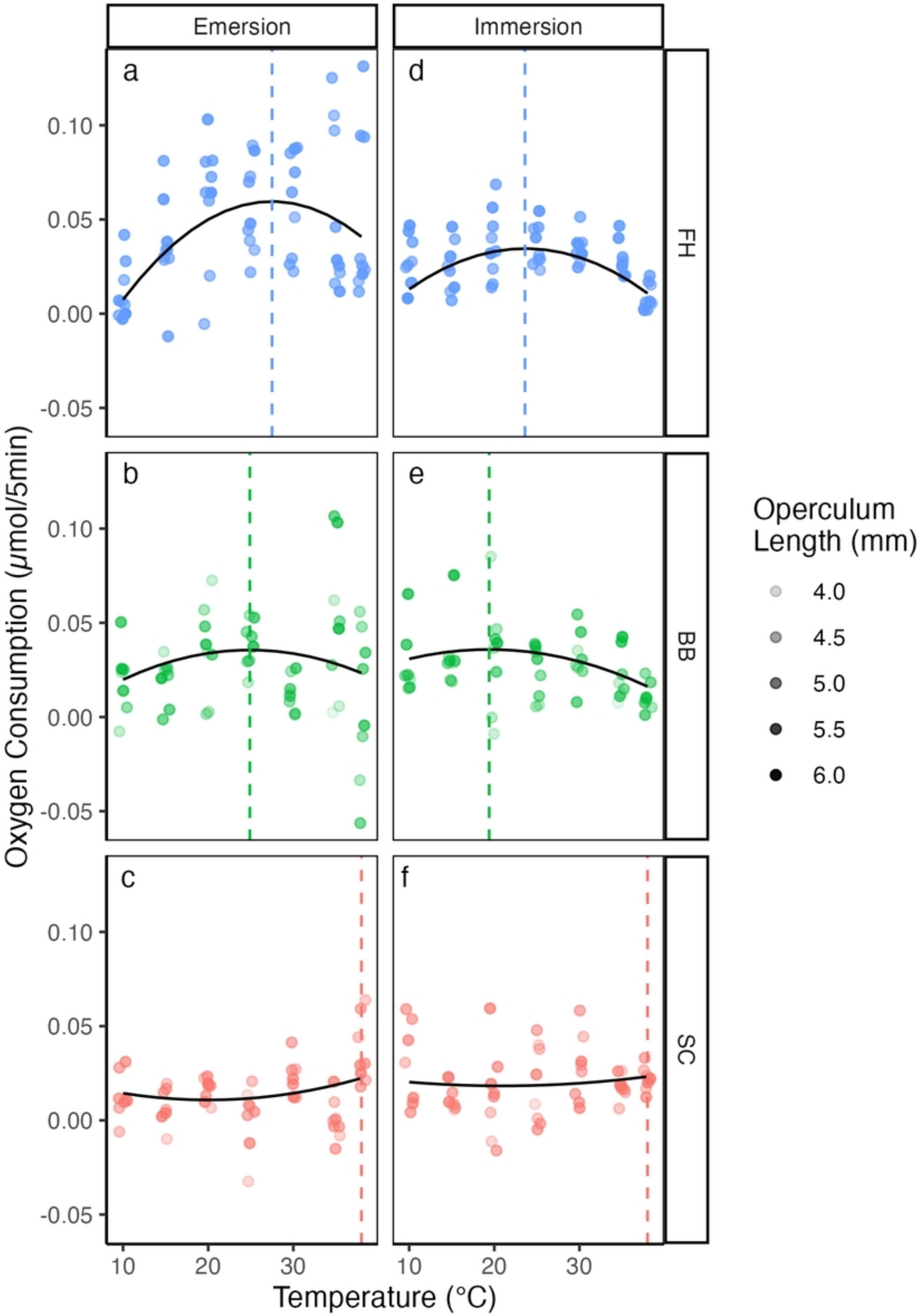
Emersion
Immersion
a
d
FH
b
e
BB
c
f
SC
0.10
0.05
0.00
-0.05
10
20
30
Temperature (°C)
Oxygen Consumption (μmol/5min)
Operculum Length (mm)
4.0
4.5
5.0
5.5
6.0

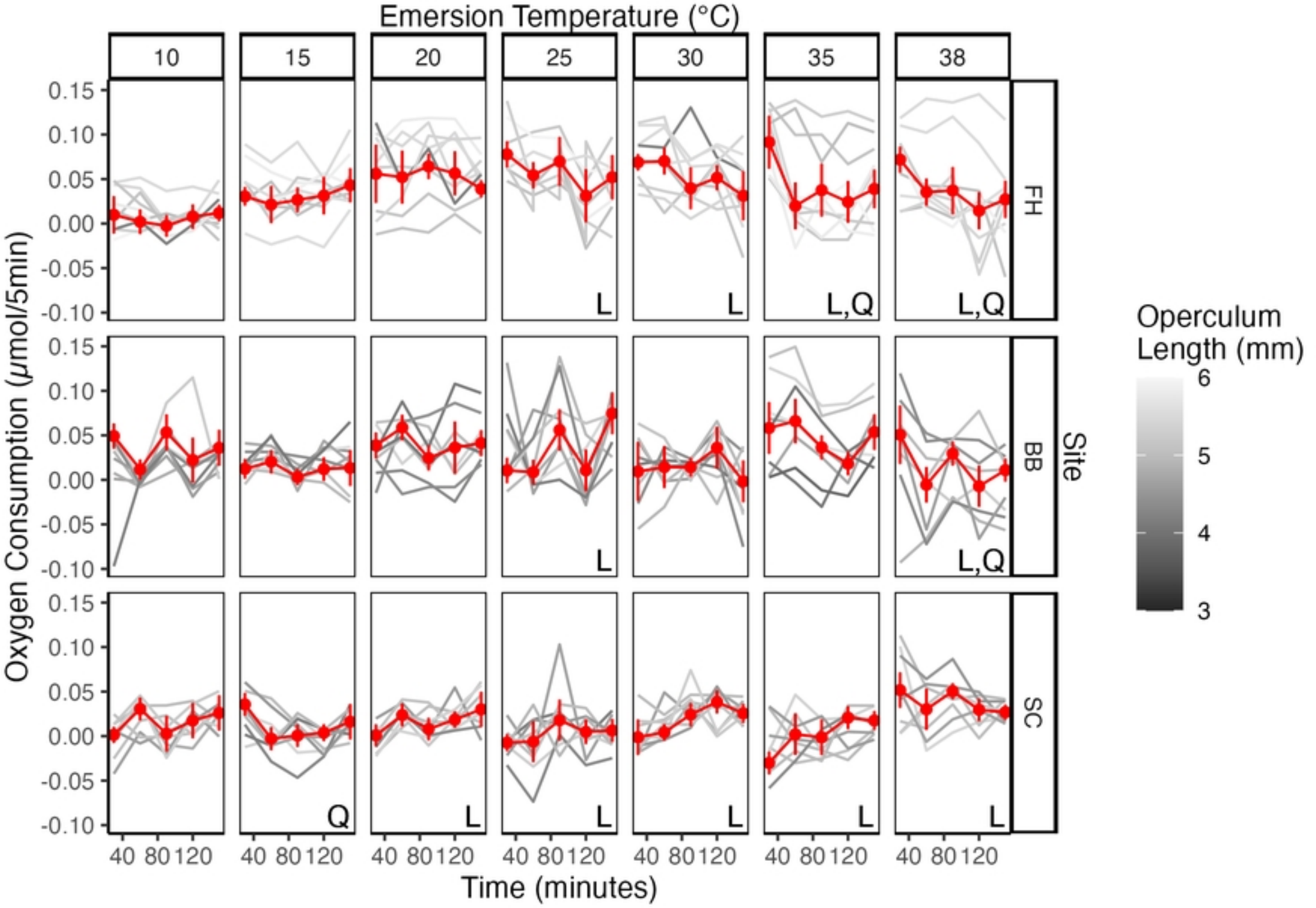
Emersion Temperature (°C)
10
15
20
25
30
35
38
Oxygen Consumption (μmol/5min)
0.15
0.10
0.05
0.00
-0.05
-0.10
FH
BB
SC
Site
L
L
L,Q
L,Q
L
L,Q
Q
L
L
L
L
L
40 80 120
Time (minutes)
Operculum Length (mm)
6
5
4
3

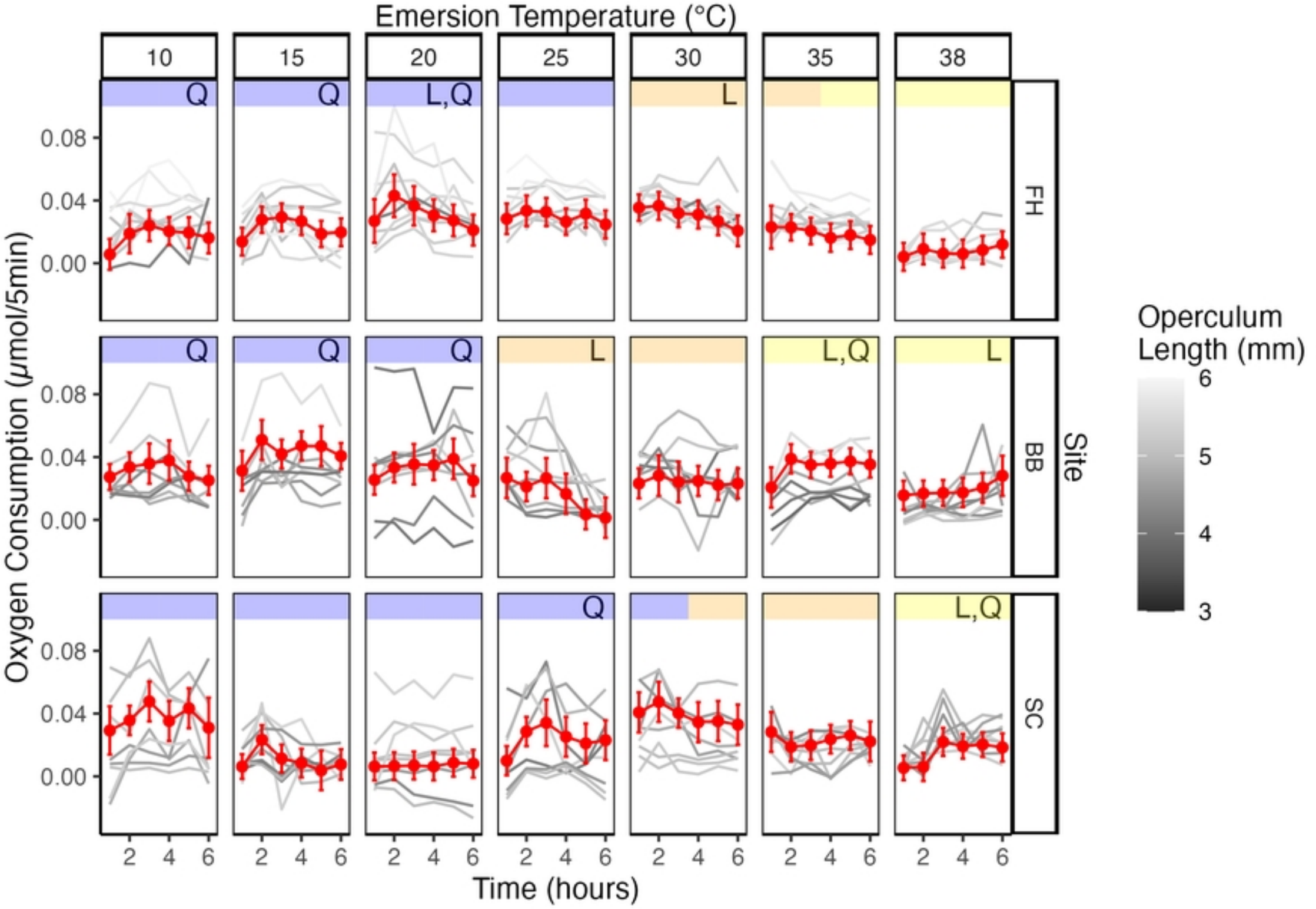
Emersion Temperature (°C)
10
15
20
25
30
35
38
Q
Q
L,Q
L
Q
Q
Q
L
L,Q
L
Q
L,Q
FH
BB
SC
Site
Oxygen Consumption (μmol/5min)
0.08
0.04
0.00
2
4
6
Time (hours)
Operculum Length (mm)
6
5
4
3

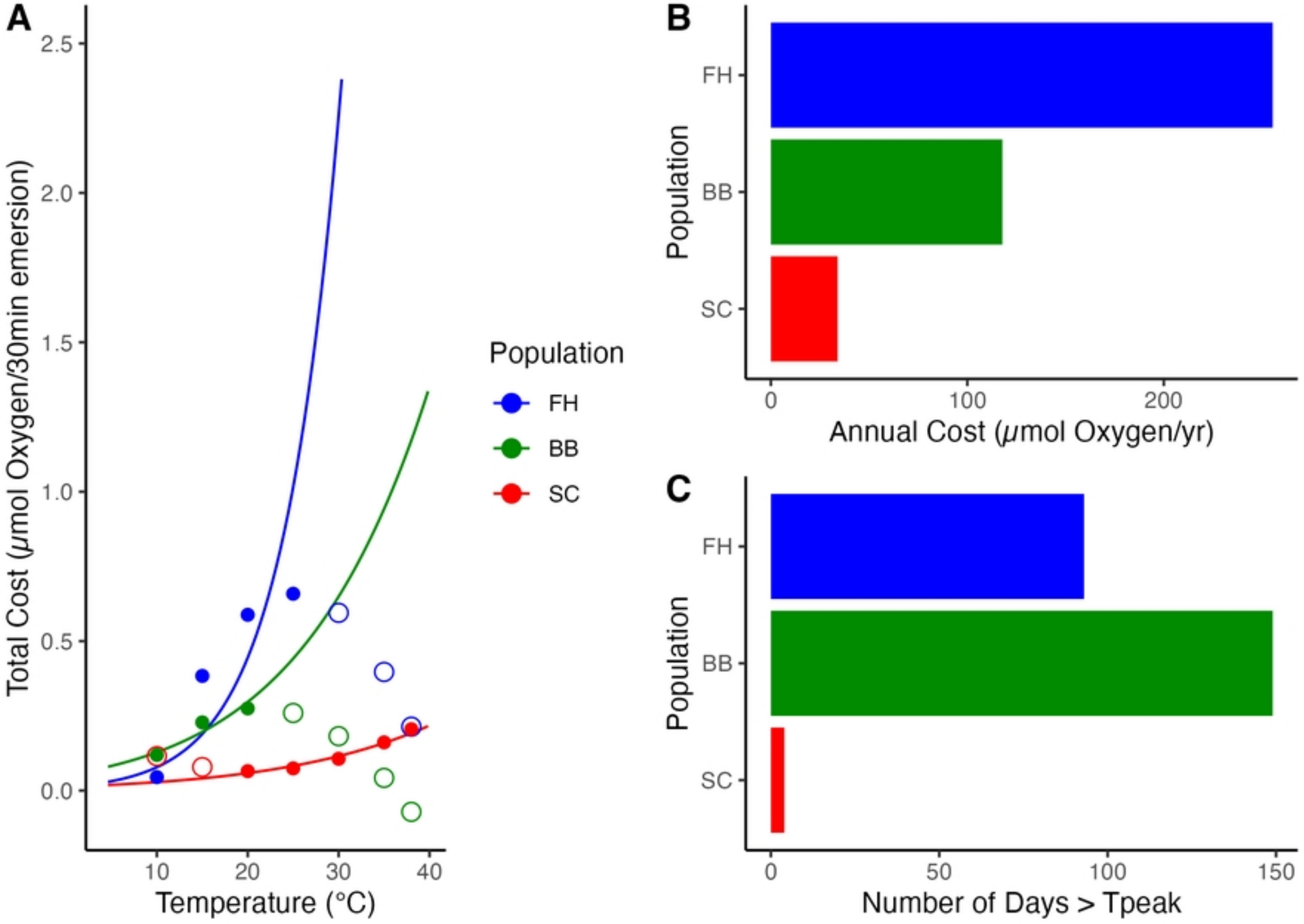
A
Total Cost (μmol Oxygen/30min emersion)
2.5
2.0
1.5
1.0
0.5
0.0
10
20
30
40
Temperature (°C)
Population
FH
BB
SC
B
Population
FH
BB
SC
0
100
200
Annual Cost (μmol Oxygen/yr)
C
Population
FH
BB
SC
0
50
100
150
Number of Days > Tpeak